Glass and Ceramics, Vol. 68, Nos. 11 – 12, March, 2012 (Russian Original, Nos. 11 – 12, November – December, 2011)

UDC 666.7

PROPERTIES OF MULLITE-ZIRCONIUM CERAMIC OBTAINED BY SPARK PLASMA SINTERING

A. V. Hmelov[1] and I. Shteins[2]

Translated from *Steklo i Keramika*, No. 12, pp. 17 – 22, December, 2011.

For ceramic samples obtained from powders after milling and synthesis in a reactor using illite clay as a binder the following were determined as a function of the temperature regime during spark plasma sintering: development of crystal phases (mullite, pseudocubic zirconium dioxide, and zircon), microstructure, linear shrinkage, apparent density, and compression strength. X-ray phase analysis showed intense development of the mullite phase and pseudocubic zirconium dioxide in all samples with increasing sintering temperature; formation of a dense microstructure of the samples is also observed. In addition, the linear shrinkage of the samples increases with increasing sintering temperature; the apparent density and compression strength of the samples also increase with milling time increasing to 24 h and introduction of clay into the samples, showing maximum values 3.45 g/cm^3 and 252.0 MPa, respectively.

Key words: spark plasma sintering, mullite-zirconium ceramic, clay, properties.

Mullite-zirconium ceramic is of interest for the manufacture of heat-proof and high-temperature ceramic materials based on it. Mullite-zirconium ceramic is characterized by high physical-mechanical properties [1, 2].

Both the conventional method of sintering [3, 4] and modern methods, for example, microwave [5] and hot or hot isostatic sintering [6], are used to obtain such ceramics. A newer pressing/sintering method has been in use in recent years — spark plasma sintering [7].

As a quite new form of pressing/sintering spark plasma sintering is more often used to obtain oxygen-free ceramics, such as TiC, TiN, WC, MoSi, Si_3N_4, ZrC, ZrB_2, and others [8 – 10], as well as single-component oxide ceramic [11]. It is indicated in a series of publications [12, 13] that a multicomponent ceramic, including mullite-zirconium, can be obtained by this method.

Aluminum, silicon, and zirconium oxides or similar mixtures containing clay are used as initial materials to obtain mullite-zirconium ceramic by spark plasma sintering [14]. A characteristic feature of such compositions is that in course of spark plasma sintering clay acts simultaneously as a flux and a source of formation and development of the mullite phase on account of the decomposition of the clay. Mixtures consisting of aluminum oxide (α-Al_2O_3) and zirconium silicate ($ZrSiO_4$) [13, 15], which at 1200°C decomposes with zirconium dioxide and silicon dioxide being formed, are also used. The mullite phase forms from such a mixture of components via the reaction [13]

$$2ZrSiO_4 + 3Al_2O_3 \rightarrow 3Al_2O_3 \cdot 2SiO_2 + 2ZrO_2.$$

In spite of its uniqueness, i.e., compaction and sintering of the ceramic powder occur together, sintering at relatively high temperatures is fast and uniform, and grain growth (i.e., recrystallization) in the ceramic powder in the course of sintering is prevented, spark plasma sintering has a number of technological and economic drawbacks: only simple sample shapes can be obtained; binding agents capable of improving the sintering of powders (for example, the introduction of Y_2O_3 or Al_2O_3 to sinter oxygen-free ceramic) must be used; the process is highly energy intensiveness; and, the generator used for the plasma discharge and the graphite mould for pressing are expensive [13, 15]. All this taken together prevents wide use of this method.

The introduction of zirconium dioxide into mullite ceramic [13] with sintering to 1500°C increases the apparent density (in the range 2.76 – 3.00 g/cm^3) and compression strength (to 275 MPa) of the samples. The maximum value of the elastic modulus at sintering temperature 1300 – 1500°C is 25.5 – 34.0 GPa [13, 15]. However, no information on the use of clay as a binder is reported in these works.

A possible mechanism [16] for the sintering of particles during spark plasma pressing consists of several stages:

– passage of electric-discharge charge through the ceramic powder and Joule heating of the powder;

[1] Riga Technical University, Institute of Silicate Materials, Riga, Latvia (e-mail: aleksejs_hmelovs@ktf.rtu.lv).
[2] Institute of Inorganic Chemistry, Salaspils, Latvia.

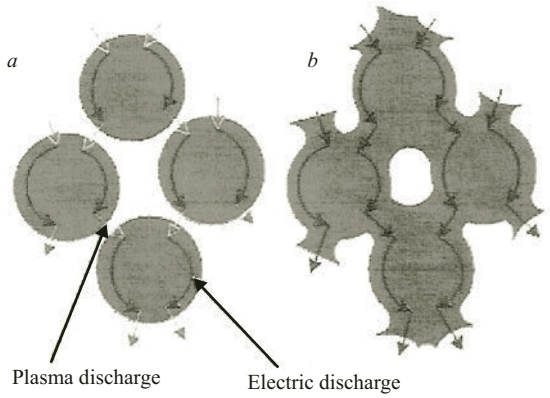

Fig. 1. Possible mechanism for sintering of particles during spark plasma pressing [16]: *a*) plasma heating of powder; *b*) intergrowth of particles with Joule heating.

– formation of plasma between the powder particles;

– intergrowth of particles (i.e., neck formation and growth) and obtaining a monolithic ceramic material (Fig. 1).

The effect of the initial ceramic powders obtained by milling and hydrothermal synthesis using components of clay as a binder on the characteristics of mullite-zirconium ceramic manufactured by the conventional methods is examined in [17, 18].

Spark plasma sintering was performed in the Model SPS-825 facility (Spark Plasma Sintering — SPS, Summimoto; CE, Dr. Sinter, Japan) (Fig. 2).

The objective of the present work is to determine the effect of spark plasma sintering on the development of crystalline phases, the microstructure, and the physical-mechanical properties of ceramic samples obtained from comminuted powders and powders synthesized by the hydrothermal method, using illite clay as the binder, in the ternary system Al_2O_3–SiO_2–ZrO_2 with Y_2O_3 addition.

The ceramic powders obtained were placed in amounts about 50 g into a 30 mm in diameter graphite mould. The sintering conditions for the ceramic powders were as follows:

– furnace medium — 6 Pa vacuum, which was held throughout the entire spark plasma pressing for a given sample;

– sintering temperature range for the ceramic samples 1150 – 1400°C;

– temperature rise rate 100°C;

– maximum pressure on the samples 30 MPa;

– soaking time at each value of the temperature 2 min.

The composition of the crystalline phases in the ceramic obtained was determined using the x-ray diffraction method (model Rigaku, Japan, with CuK_α radiation, scanning interval $2\theta = 10 – 60°$, scanning rate 4 K/min) after each heat cycle of sintering. The microstructure of the ceramic samples, dimensions, and morphology of the crystalline particles were determined using a scanning electron microscope (SEM, model JSM-T200, Japan).

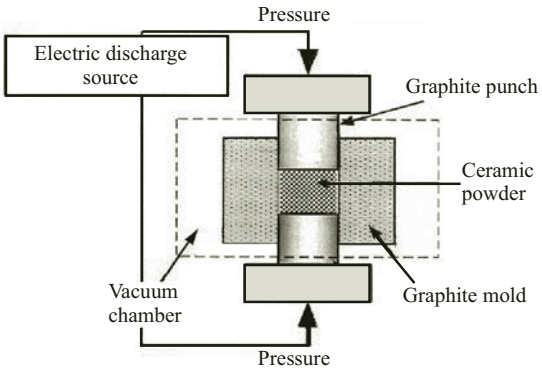

Fig. 2. Schematic diagram of the spark plasma sintering facility [19].

The apparent density was found from the ratio of the mass of a dry sample to the mass of a sample immersed in distilled water (i.e., to its volume) according to the standard EN LVS 63-01:2001:

$$\rho_{app} = g_0 / g_2 ,$$

where ρ_{app} is the apparent density, g/cm^3; g_0 is the mass of the dry sample, g; g_2 is the mass of the sample immersed in water, g (ρ_{H_2O} = ~ 1 g/cm^3 at $T = 22 \pm 2$°C).

The linear shrinkage of the samples was determined from the dimensions of the sample before and after spark plasma sintering following the standard EN LVS 63-01:2001 according to the relation

$$\Delta l = \frac{l_0 - l_1}{l_0} \times 100,$$

where Δl is the linear shrinkage of the sample, %; l_0 is the size of the sample before spark plasma sintering, mm; and, l_1 is the size of the sample after spark plasma sintering, mm.

The compression strength of the ceramic samples was determined according to the standard EN 568-2:2003 using the TONI Technic Controller TT 0995 facility. Before the compression strength tests were performed the surfaces of the samples to which load was applied were carefully polished.

In the present work the development of crystalline phases in ceramic samples obtained by spark plasma sintering from comminuted powders and powders synthesized by the hydrothermal methods in the temperature range from 1200 to 1400°C, which is shown in the x-ray diffraction pictures (Fig. 3), was investigated.

The x-ray diffraction patterns (Fig. 3*a* and *b*) indicate intense formation and development of a mullite phase as well as pseudocubic zirconium dioxide, especially at temperature 1400°C. This is explained by the presence of yttrium oxide Y_2O_3 addition in the initial powder, which not only promotes a transition from tetragonal into pseudocubic [20] zirconium dioxide but also nucleation and formation of a mullite phase

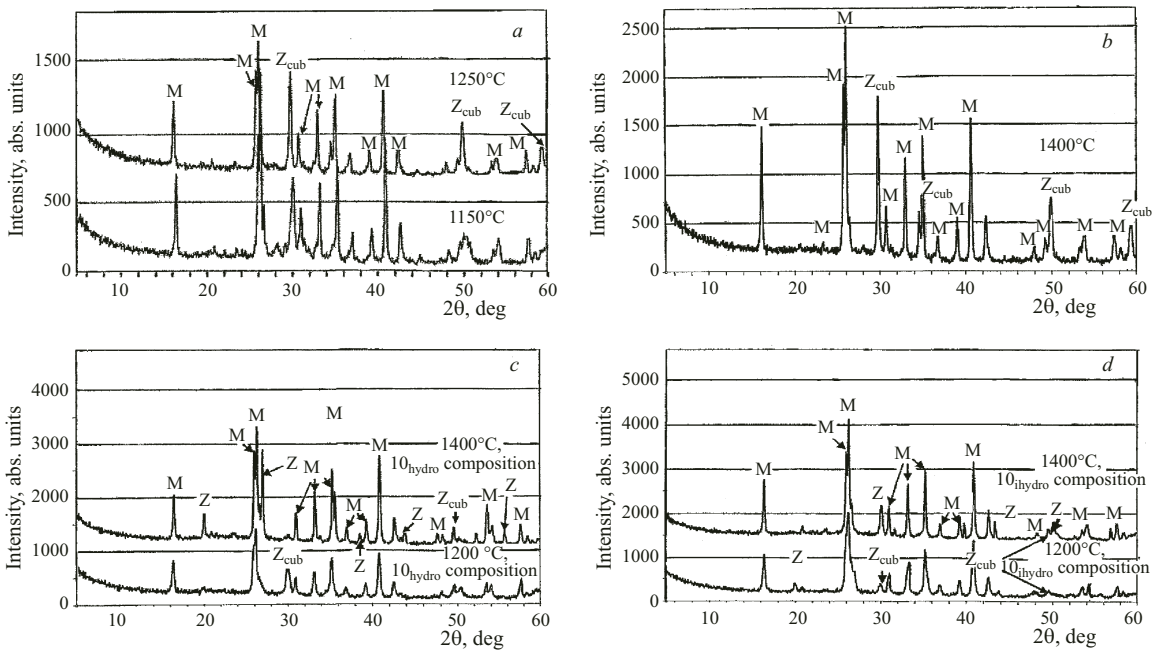

Fig. 3. X-ray phase analysis of ceramic samples sintered by the spark plasma method from powder after milling for 24 h (*a*, *b*) and powders after synthesis in a reactor (*c*, *d*) in the temperature range 1150 (1200) – 1400°C, respectively: M) mullite ($3Al_2O_3 \cdot 2SiO_2$), Z_{cub}) pseudocubic ZrO_2, Z) zircon ($ZrSiO_2$), hydro (ihydro)) hydrothermal synthesis (hydrothermal synthesis with clay addition).

owing to the development of solid solutions based on aluminum oxide with yttrium oxide starting from 1150 to 1400°C.

Likewise, at relatively low temperatures in samples (starting at 1150 (1200)°C) pseudocubic zirconium dioxide forms owing to the presence of the vacuum in which spark plasma sintering occurs, forming quite stable solid solutions based on ZrO_2 with Y_2O_3, since at atmospheric pressure similar solid solutions form in the temperature interval 1900 – 2100°C.

At the same time a similar tendency is observe in samples (Figs. 3c, d) obtained from powders synthesized in an autoclave, but some differences are noted. The x-ray diffraction patterns show intensification of the diffraction peaks of mullite and a decrease in the amount of pseudocubic zirconium dioxide. The decomposition of aluminosilicate (similar to the mineral sillimanite) at temperature about 1000°C and the conversion (i.e., transformation) of clay minerals in the course of hydrothermal synthesis promote intense formation of mullite during spark plasma sintering. In addition, zircon formation is observed. From the practical standpoint this is an unwanted phenomenon for mullite-zirconium materials for the following reasons:

– the fire-resistance of the materials decreases because silicon dioxide, which is necessary for mullitization, is consumed;

– the operational temperature of refractories decreases because zircon decomposes (1400°C) and then silicon dioxide melt, which corrodes the refractory, is released.

In the present case, judging from the intensities of the diffraction peaks of mullite, this effect is not so strongly expressed because of the effect of excess [17] yttrium oxide in the initial compositions. The presence of clay also affects the formation of zircon. As Fig. 3*d* shows, the amount of zircon in the compositions with clay addition decreases considerably at the same incidence/reflection angles of the x-ray beam (2θ ~ 28.52°) compared with the analogous sample with no clay, because the clay apparently acts as a flux in the sintered powder, thereby slowing down zircon formation.

The crystalline phases and the ensuing microstructure change of the samples are observed in the results obtained with the SEM (Fig. 4).

The studies showed differences in the microstructures of the samples, sintered by the spark plasma method, and synthesized initial powders obtained by different methods.

In the first case (Fig. 4*a*), a uniform, dense, crystalline microstructure, in which uniformly distributed grains of pseudocubic zirconium dioxide are observed, is formed. The mullite crystals are very small, only 1 – 2 μm in size.

The microstructure of a sample sintered from powder synthesized in a reactor is amorphous-like (Fig. 4*b*).

Pseudocubic zirconium dioxide is observed in small quantities. The main difference of this microstructure is the presence of incompletely formed (i.e., xenomorphic) mullite crystals, which is due to the decomposition of aluminosilicate — sillimanite — in the course of spark plasma sintering.

The increase of linear shrinkage (i.e., change of dimensions along height) of the samples as a function of the sintering temperature is shown in Fig. 5.

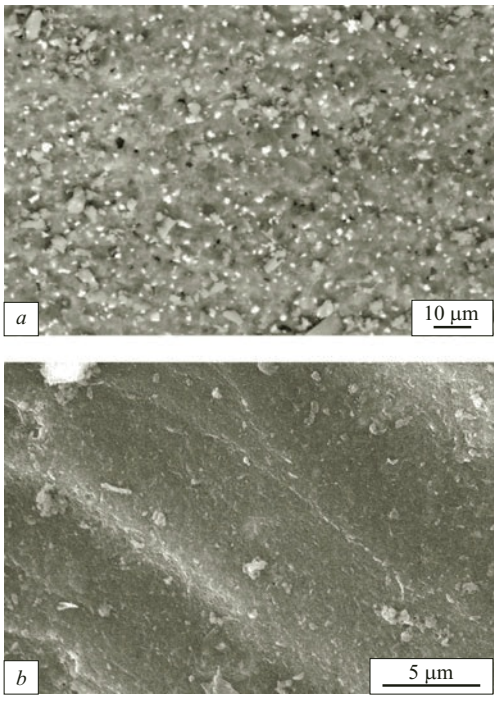

Fig. 4. Microstructure of ceramic samples after spark plasma sintering at 1300°C, obtained from comminuted powder, with 24 h milling (*a*) and powder after hydrothermal synthesis (*b*): mullite crystals (dark phase) and pseudocubic zirconium dioxide (white grains).

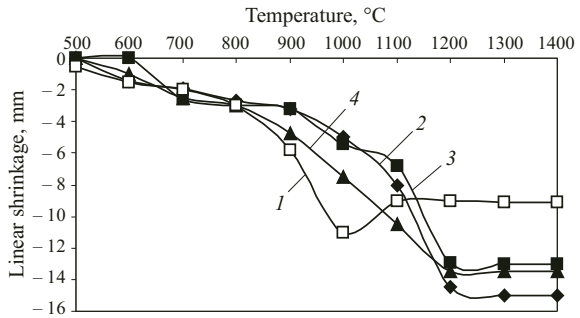

Fig. 5. Development of linear shrinkage of samples in the course of spark plasma sintering in the temperature range 500 – 1400°C: *1*) hydrothermal synthesis; *2*, *3*, *4*) powder milling time 4, 12, 24 h, respectively.

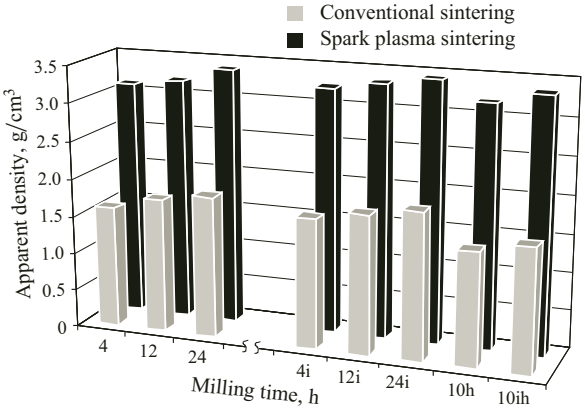

Fig. 6. Change of the apparent density of ceramic samples sintered by two methods — conventional and by spark plasma sintering at 1300°C: i) samples with illite clay addition; h) hydrothermal synthesis, samples with no clay; ih) hydrothermal synthesis with illite clay addition.

The results of linear shrinkage of the samples sintered from powders after milling differ little from one another, irrespective of the milling time. As expected, the most intense development of linear shrinkage is seen in the temperature interval from 800 to 1200°C in the sample sintered from powder after 24 h milling, reaching maximum shrinkage (45.0%) at 1200°C, which subsequently remains unchanged because of the formation of a quite completely sintered sample. Slower sintering at temperatures from 1100 to 1200°C is seen for samples sintered from powders after milling for 4 and 12 h. This is due to the lower activity of the particles and the presence of large particles in the comminuted powders [17]. Nonetheless, these samples at 1200°C also show high linear shrinkage 48.3 and 43.0%, respectively. The additional linear shrinkage of the sample (after 4 h milling) at temperature to ~1250°C is related with the compaction of large particles, but on the whole the sintering process is already complete at this stage.

The sample made from powders of hydrothermal origin shows an interesting dependence of the linear shrinkage on the sintering temperature. At first the changes of the linear shrinkage to 900°C appear in a similar manner, just as in the case of sintering of samples obtained from comminuted powders. But, at temperatures from 900°C to 1000°C the linear shrinkage increases sharply to 36.7%. This is because the initial powder after hydrothermal synthesis contains agglomerates which under the pressure of the load start to break down in the course of spark plasma sintering, forming smaller and more active particles giving rise to sintering of the powder. However, the reverse effect appears at temperatures from 1000 to 1100°C — the linear shrinkage of the sample decreases because of the agglomeration of the newly formed particles in the powder and then remains unchanged.

Likewise, the apparent density and compression strength of the samples increase in parallel with the linear shrinkage (Figs. 6 and 7).

In Fig. 6 the apparent density of a sample sintered by different methods differs considerably. For example, the apparent density of the samples sintered under the influence of a plasma discharge from powders after 24 h milling with illite clay addition reaches 3.45 g/cm^3, which, evidently, is several-fold greater than that (1.94 g/cm^3) of the sample sintered conventionally and containing clay. This is explained by the more active "overgrowth" of closed pores during spark plasma sintering. In spite of this, the tendency for the apparent density to increase with increasing milling time, i.e., dispersity of the powder, irrespective of the sintering

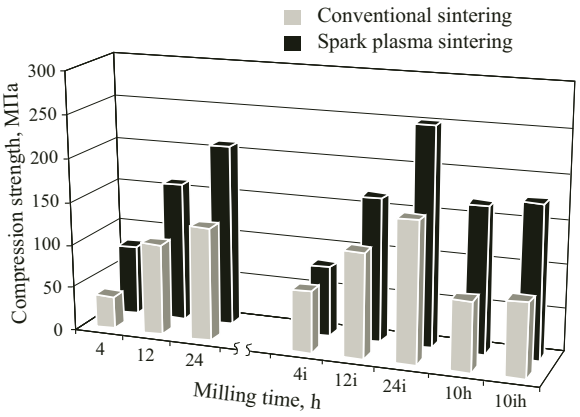

Fig. 7. Change of the compression strength of ceramic samples sintered by two methods — conventional and by spark plasma sintering at 1300°C: i) samples with illite clay addition; h) hydrothermal synthesis, samples with no clay; ih) hydrothermal synthesis with illite clay addition.

method is uniform in all samples. The fact that the apparent density of the samples (10h and 10ih) is lower than that of samples sintered from comminuted powders is probably due to the high crystallinity of the hydrothermal powders.

The change of the compression strength (Fig. 7) of the samples as a function of the analogous parameters has a tendency to increase, only more rapidly and especially with clay additive.

The highest compression strength of the samples corresponds to the longest milling time, including for samples obtained from powders by the hydrothermal method. At the same time an increase of compression strength of the sample (24i) with illite addition is very considerable, reaching the maximum value 250 MPa, compared with the sample (162 MPa) sintered conventionally. Such high compression strength is due to the development of a quite uniform dense microstructure (see Fig. 4*a*); a clay addition also has an effect associated with its amorphization and formation of new grain shapes during prolonged milling, which has a catalytic effect, i.e., accelerates sintering at the initial stage at temperatures from 600 to 750°C, and at 1300°C the clay particles act as natural nanomaterials or so-called nanoreactors.

Conversely, the samples sintered conventionally are characterized by lower compression strength because the recrystallization of mullite crystals is more complete and because of the crystallinity of the particles in the powder synthesized by the hydrothermal method.

The effect of spark plasma sintering on the formation and development of the mullite phase and pseudocubic zirconium dioxide in the samples with and without clay addition was studied in the present work. The changes due to the formation of the microstructure of sintered samples were analyzed. Likewise, the regularities in the development of linear shrinkage of the samples as a function of the temperature regime of spark plasma sintering were determined and a relation was established between the apparent density and the compression strength of the samples.

The development of a mullite phase and pseudocubic zirconium dioxide with increasing sintering temperature was found in the samples sintered from powders after milling. A similar tendency is also observed for samples obtained from hydrothermally synthesized powders. The clay and yttrium oxide additions in these samples as well as the vacuum medium also promote the development of a mullite phase and pseudocubic zirconium dioxide, and a decrease of zircon in the samples with clay is observed.

The microstructure of both samples is quite dense, but for the sample obtained from powder after hydrothermal synthesis an amorphously similar microstructure is observed. Improvement and crystallization of mullite crystal is clearly seen in samples obtained from powders by the conventional method, compared with the sample obtained from powder after hydrothermal synthesis.

The linear shrinkage increases in all samples sintered from powders after milling right up to temperature 1200 (1250)°C. At the same time the increase of the linear shrinkage for samples sintered from hydrothermal powders is sharper at temperatures 900 – 1000°C. This can be explained by the "breakdown" of agglomerates with new, small, active particles being formed.

The changes in the apparent density are uniform for all samples, increasing somewhat for samples with clay addition. The compression strength increases most rapidly for samples with clay addition, on which the microstructure and clay addition have a positive effect, especially after 24 h milling. Samples sintered conventionally and by the spark plasma method from powders synthesized by the hydrothermal method show lower apparent density and lower compression strength.

REFERENCES

1. P. P. Budnikov and D. N. Poluboyarinov, *Chemical Technology of Ceramics and Refractories* [in Russian], Literatura po stroitel'stvu, Moscow (1972).
2. I. É. Spherberga, G. U. Sedmalis, and G. P. Sedmale, *Physical Chemistry of Silicates and Refractory Nonmetallic Compounds* [in Russian], RTU, Riga (2010).
3. Y. Lin and Y. Chen, "Fabrication of mullite composites by cyclic infiltration and reaction sintering," *Mat. Sci. Eng. A*, **298**, 179 – 186 (2001).
4. H. C. Park, T. Y. Yang, and S. Y. Yoon, "Preparation of zirconia-mullite composites by an infiltration route," *Mat. Sci. Eng. A*, **405**, 2333 – 2338 (2005).
5. P. Piluso. L. Gaillard, N. Lequeux, and P. Boch, "Mullitisation and densification of ($3Al_2O_3 + 2SiO_2$) powder compacts by microwave sintering," *J. Eur. Ceram. Soc.*, **16**(2), 121 – 125 (1996).
6. S. Hartmut and S. Komarneni, *Mullite*, Technology and Engineering, N.Y. (2005), pp. 130 – 131.
7. R. Sivakumar, D. D. Jayaseelan, T. Nishikawa, et al., "Influence of MgO on microstructure and properties of mullite – Mo com-

posites fabricated by pulse electric current sintering," *Ceram. Int.*, **27**(5), 537 – 541(2001).
8. F. Guillard, A. A. Hemand, J.-D. Lubewicz, and J. Galy, "Densification of SiC by SPS-effects of time, temperature and pressure," *J. Eur. Ceram. Soc.*, **27**(7), 2725 – 2728 (2001).
9. A. Ragulya, V. Kolesnichenko, and M. Herrmann, "Structure and properties of spark-plasma sintered TiN – Si_3N_4 ceramic nanocomposites reinforced with Si_3N_4 nanowires," in: *Abstracts of Reports at the 3rd International Congress on Ceramics* (2010).
10. N. Gupta, R. M. Reddy, K. Pavani, and B. Basu, "Multi-stage spark plasma sintering to develop ZrB_2 – 18 wt% SiC – *x* wt% $TiSi_2$ composites with better properties," in: *Abstracts of Reports at the 3rd International Congress on Ceramics* (2010).
11. K. A. Khor, L.-G. Yu, S. H. Chan, and Y. J. Chen, "Densification of plasma sprayed YSZ electrolytes by spark plasma sintering (SPS)," *J. Eur. Ceram. Soc.*, **23**(11), 1855 – 1863 (2003).
12. K. A. Khor, L. G. Yu, Y. Li, et al., "Spark plasma reaction sintering of ZrO_2 – mullite composites from plasma spheroidized zircon – alumina powders," *Mat. Sci. Eng.*, **339**(1 – 2), 286 – 296 (2003).
13. E. Rocha-Rongel and H. Miyamoto, "Zirconia-mullite composites consolidated by spark plasma reaction sintering from zircon and alumina," *J. Am. Ceram. Soc.*, **88**(5), 1150 – 1157 (2005).
14. I. Sperberga, A. Hmelov, G. Sedmale, and A. Pludons, "Contribution of spark plasma sintering to the development of mullite – ZrO_2 ceramics," *Chemine Technol.*, **50**(1), 61 – 64 (2009).
15. G. Jin, M. Takeuchi, S. Honda, et al. "Properties of multilayered mullite/Mo functionally graded materials fabricated by powder metallurgy processing," *Mat. Chem. Phys.*, **89**(2 – 3), 238 – 243 (2005).
16. http://www.Substech.com/spark plasma sintering/scheme/htm.
17. A. V. Hmelov, G. P. Sedmale, and I. É. Sperberga, "Effect of dispersity of ceramic powders on the properties of mullite-zirconium ceramic," *Novye Ogneupory*, No. 1, 41 – 46 (2011).
18. A. V. Hmelov and G. P. Sedmale, "Characteristics of mullite-zirconium ceramics obtained from powders synthesized by the hydrothermal method," *Steklo Keram.*, No. 4, 22 – 26 (2011); G. P. Sedmale and A. V. Hmelov, "Characteristic of mullite-zirconium ceramic obtained from powders synthesized by the hydrothermal method," *Glass Ceram.*, **68**(3 – 4), 123 – 127 (2011).
19. T. Murakami, J. H. Ouyang, S. Sasaki, et al., "High-temperature tribological properties of spark-plasma-sintered Al_2O_3 composites containing barite-type structure sulfates," *Tribology Int.*, **40**(2), 246 – 253 (2007).
20. N. A. Toropov, V. P. Barzakovskii, V. V. Lapin, and N. N. Kurtseva, "Pseudocubic ZrO_2 — solid solution based on cubic ZrO_2 with Y_2O_3 according to the binary phase diagram of the system ZrO_2–Y_2O_3," in: *Handbook of Phase Diagrams of Silicate Systems — Binary Systems* [in Russian], Nauka, Leningrad (1969), Vol. 1, pp. 437 – 439.